Biomedical Research 2017; 28 (19): 8260-8266 *ISSN 0970-938X*
www.biomedres.info

Utility of $^{99m}TcO_4^-$ static imaging for detecting metastatic lesions in differentiated thyroid cancer.

Hongbo Gao[1#], Wei Song[1#], Yuqing Di[1], Haichun Liu[1], Yujun Shao[1], Linlin Ma[1], Zheng Li[1], Congjun Jin[1], Huiliang Xie[1], Chunyuan Zhao[1], Lijun Yang[1], Xiaoyong Zhang[1*], Yonghui Chen[2*]

[1]Department of Radionuclide Treatment Center, Beijing 401 Hospital of Chinese Nuclear Industry, Beijing, PR China

[2]Department of Nuclear Medicine, Peking Union Medical College Hospital, Chinese Academy of Medical Sciences and Peking Union Medical College, Beijing, PR China

[#]These authors contributed equally to this work

Abstract

The aim of this study was to evaluate the utility of thyroid static imaging with $^{99m}TcO_4^-$ for detecting metastatic lesions following surgery in patients with Differentiated Thyroid Cancer (DTC). A total of 420 consecutive post-total thyroidectomy patients with pathologically diagnosed differentiated thyroid cancer underwent thyroid static imaging with $^{99m}TcO_4^-$ before ^{131}I treatment to evaluate the size, location, and function of the residual thyroid. They also underwent ^{131}I whole-body scanning (^{131}I-WBS), as well as single-photon emission computed tomography/computed tomography fusion imaging (when necessary), for evaluation of the lesions. The detection rates of thyroid static imaging with $^{99m}TcO_4^-$ and ^{131}I-WBS (therapeutic dose) were 83.81% and 98.33%, respectively. The sensitivity of $^{99m}TcO_4^-$ thyroid static imaging was 85.2%, and the rate of detection with both $^{99m}TcO_4^-$ static imaging and ^{131}I-WBS was 85.48%. The use of $^{99m}TcO_4^-$ thyroid static imaging identified metastatic lesions in 10 patients; thus, the original planned treatment dose and protocol were adjusted in these patients. Based on our findings, we conclude that thyroid static imaging with $^{99m}TcO_4^-$ can be used to evaluate the residual thyroid tissue after thyroid carcinoma resection and can identify metastatic lesions, thereby helping to guide the selection of the ^{131}I treatment dose.

Keywords: Differentiated thyroid carcinoma, $^{99m}TcO_4$-thyroid static imaging, ^{131}I whole body scanning.

Accepted on September 11, 2017

Introduction

Thyroid carcinoma is the most common malignant tumor of the endocrine system, out of which more than 90% are cases of Differentiated Thyroid Carcinomas (DTCs). Total thyroidectomy or near total thyroidectomy combined with ^{131}I thyroid remnant ablation, as well as thyroid hormone suppressive therapy, is the main approach recommended by the current treatment guidelines for DTC [1]. To understand the patients' surgical conditions and to determine the optimal ^{131}I dose before treatment, it is often necessary to evaluate the size, location, and function of the residual thyroid tissue.

Although ^{123}I imaging is commonly used to evaluate the residual thyroid tissue worldwide, it is both expensive and difficult to access in China [2-4]; therefore, ^{131}I imaging is used as an alternative. However, some researchers consider that small doses of ^{131}I can cause the so-called "stunning" phenomenon observed in diagnostic imaging [3,5] and that this phenomenon alters the ultimate therapeutic effect. In contrast, other researchers have reported that thyroid stunning has no effect on the therapeutic outcome [6,7]. Therefore, it is necessary to identify the most suitable imaging agent to assess the residual thyroid tissue.

Because $^{99m}TcO_4^-$ can appropriately reflect the sodium iodide symporter (NIS) expression [8,9], thyroid static imaging with $^{99m}TcO_4^-$ is often used clinically to assess the size, location, and function of the residual thyroid tissue. Although several studies have reported that $^{99m}TcO_4^-$ thyroid static imaging can occasionally detect metastatic thyroid cancer, owing to its limited sensitivity as well as the fact that its diagnostic capacity may depend on high levels of Thyroid-Stimulating Hormone (TSH) in stimulated states, this approach is not widely used [10-12].

Moreover, some studies have shown that $^{99m}TcO_4^-$ systemic scanning can reveal metastatic DTC lesions in the neck and chest [13], while other studies have revealed that $^{99m}TcO_4^-$ thyroid static imaging cannot only accurately assess the size, location, and function of residual thyroid tissue but that, in some cases of DTC, it can also reveal metastatic lesions, such as lymph node, lung, or bone metastases, thereby helping

physicians to promptly adjust the patients' clinical stages and modify their treatment plans.

The presence of NIS protein is the underlying mechanism for the uptake of ^{131}I and $^{99m}TcO_4$ by cancer tissues. However, it is unclear why $^{99m}TcO_4^-$ thyroid static imaging can only reveal metastatic lesions in certain types of DTC, instead of in all types. This may be the result of high NIS expression in the detected metastatic lesions. Lesions with high expression of NIS are also likely to have high ^{131}I uptake ability, implying a good therapeutic effect with ^{131}I and consequently a better prognosis.

In the present study, we aimed to investigate whether metastatic lesions of DTC detected *via* $^{99m}TcO_4^-$ thyroid static imaging respond well to ^{131}I therapy, and whether patients with these lesions have a better prognosis. The main objective of the study was to determine whether $^{99m}TcO_4^-$ thyroid static imaging can be used as an alternative to ^{131}I imaging for the evaluation of ^{131}I treatment. The traditional approach is to use small doses of ^{131}I diagnostic imaging for preoperative evaluations; however, as mentioned above, the use of this method is limited due to controversy regarding thyroid stunning. On the other hand, the use of $^{99m}TcO_4^-$ imaging will not result in stunning, with the advantages of high sensitivity and specificity and low radiation dosage. Thus, we moreover aimed to determine the clinical value of $^{99m}TcO_4^-$ thyroid static imaging, and whether it has unique advantages over other imaging methods.

Materials and Methods

Subjects

A total of 420 consecutive post-total-thyroidectomy patients with pathologically diagnosed DTC who underwent ^{131}I therapy from March 2014 to September 2015 in the Beijing 401 Hospital of the Chinese Nuclear Industry were selected and retrospectively analysed. Prior to treatment with ^{131}I, $^{99m}TcO_4^-$ thyroid static imaging was performed to evaluate the size, location, and function of the residual thyroid tissue, and if any abnormal findings were observed, Single-Photon Emission Computed Tomography/Computed Tomography (SPECT/CT) fusion imaging was also performed. After ^{131}I treatment, ^{131}I Whole-Body Scanning (^{131}I-WBS) and SPECT/CT fusion imaging were performed for comparison.

The data of the 420 patients showed that $^{99m}TcO_4^-$ thyroid static imaging demonstrated areas of abnormal $^{99m}TcO_4^-$ concentration in 10 patients before ^{131}I treatment (3 men and 7 women, age range 19-59 y). There were 8 cases of papillary thyroid carcinoma (including 3 cases of the follicular variant of papillary thyroid carcinoma and 2 cases of thyroid follicular carcinoma). Among these, ^{131}I-WBS, SPECT/CT fusion imaging, and sonography confirmed lymph node metastases in 7, lung metastases in 4, and bone metastasis in 1, with simultaneous lymph node and lung metastases present in 2 patients.

This study was conducted in accordance with the declaration of Helsinki. This study was conducted with approval from the Ethics Committee of Beijing 401 Hospital. Written informed consent was obtained from all participants.

$^{99m}TcO_4^-$ thyroid static imaging

A total of 185 MBq (5 mCi) of $^{99m}TcO_4^-$ (Atom Hitech Co., Ltd., Beijing, China) was intravenously injected, followed by thyroid static imaging 20 min later. Each patient was placed in the supine position with normal head position and the neck raised to fully expose the thyroid. Normal anteposition images were collected using a SIEMENS e.cam SPECT instrument (Siemens Medical Solutions USA, Inc., Malvern, PA, USA) and a Philips BrightView XCT (Philips Medical Systems, Cleveland, OH, USA) SPECT/CT instrument (equipped with low-energy high-resolution collimators). The matrix was 256 × 256 and the acquisition count was 150 k. Any foci outside the thyroid that showed obvious ^{131}I uptake, as well as lesions with evaluation and quantification difficulties, were further evaluated with SPECT/CT fusion imaging.

^{131}I-WBS

Each patient was orally administered 3.7-7.4 GBq (100-200 mCi) of ^{131}I (Atom-Hitech Co., Ltd.) after fasting and underwent ^{131}I-WBS 3 d later. During the procedure, each patient was placed in the supine position with a normal head position and the neck raised, with the hands placed on along the side of the body. SPECT and SPECT/CT (bed-moving speed 12 cm/min, equipped with high-energy universal collimators) were used for acquisition. The matrix was 256 × 1024. Any obvious foci outside the thyroid showed obvious ^{131}I uptake, as well as lesions with qualification and quantification difficulties, were subjected to further ^{131}I SPECT/CT fusion imaging.

Image analysis

Two nuclear medicine physicians interpreted the films using the double-blind method; when the conclusions were not consistent, they re-read the films together and arrived at a consensus through discussion. The following image diagnostic criteria were applied: (1) to determine whether the results of the two imaging methods were consistent, the existence of a radiation uptake focus in the cervical thyroid area was diagnosed as positive; (2) to determine films with abnormalities, the residual thyroid and physiological uptake were diagnosed as negative, while abnormal uptake in the lymph nodes, lungs, bones, and other parts was diagnosed as positive.

Results

Imaging results

The results of the two imaging methods are shown in Table 1. The detection rates of $^{99m}TcO_4^-$ thyroid static imaging and ^{131}I-WBS (therapeutic dose) were 83.81% (352/420) and 98.33%

(413/420), respectively. The sensitivity of $^{99m}TcO_4^-$ thyroid static imaging was 85.2% (352/413), and the rate of detection *via* both $^{99m}TcO_4^-$ thyroid static imaging and ^{131}I-WBS was 85.48% (359/420).

Table 1. *Results of DTC by two imaging methods (n).*

$^{99m}TcO_4^-$ thyroid static imaging	131I-WBS		Sum
	Positive	Negative	
Positive	352	0	352
Negative	61	7	68
Sum	413	7	420

Analysis of $^{99m}TcO_4^-$ static imaging

Among the 420 patients, 10 patients were found to have lesions with abnormal uptake by $^{99m}TcO_4^-$ static imaging. These were confirmed as metastases by ^{131}I-WBS, SPECT/CT fusion imaging, and ultrasound after treatment; the incidence was 2.38% (10/420), and the cancer types specifically involved were papillary thyroid cancer in 8 cases, the follicular variant of papillary thyroid carcinoma in 3 cases, and thyroid follicular carcinoma in 2 cases. Lymph node, lung, and bone metastases were present in 7, 4, and 1 case, respectively; among these, lymph node and lung metastases occurred simultaneously in 2 cases.

The original planned therapeutic dose was modified in these 10 patients according to the $^{99m}TcO_4^-$ static imaging results. The originally planned ^{131}I treatment dose was 100 mCi; patients 1-9 and 10 instead received 150 and 200 mCi of ^{131}I for thyroid remnant or lesion ablation, respectively. Surgical management of the lymph nodes was recommended for patients 1-5 after ^{131}I treatment, with a potential requirement for secondary surgery in some patients, while multiple ^{131}I lesion scavenging was recommended for patients 6-10 (Table 2).

Table 2. *Clinical data of the 10 DTC patients with metastatic lesions revealed by $^{99m}TcO_4^-$ static imaging.*

No	Gender	Age (y)	Pathological type	Abnormalities in $^{99m}TcO_4$ imaging	Abnormalities in ^{131}I-WBS	^{131}I SPECT/CT fusion imaging
1	M	30	Thyroid papillary carcinoma	Punctiform radioactive concentration area on the right clavicle	Equivalent to one punctiform abnormal intake focus on the right clavicle	Abnormal intake focus on the right clavicle, considered to be lymph node metastasis
2	M	35	Thyroid papillary (follicular carcinoma variant)	Punctiform radioactive concentration area on the sternal plane	Equivalent to one punctiform abnormal intake focus on the superior sternal fossa	Abnormal intake focus on the superior sternal fossa, considered to be lymph node metastasis
3	F	44	Thyroid papillary carcinoma	Punctiform radioactive concentration area on the superior sternal fossa	Equivalent to one punctiform abnormal intake focus on the superior sternal fossa	Abnormal intake focus on the superior sternal fossa, considered to be lymph node metastasis
4	M	49	Thyroid papillary carcinoma	Multiple punctiform radioactive concentration areas on the upper mediastinal area	Multiple punctiform and lumpy abnormal intake foci on the upper mediastinal area	Abnormal intake foci on the upper mediastinal area, considered to be lymph node metastasis
5	F	26	Thyroid papillary carcinoma	Multiple punctiform radioactive concentration area on the left lateral neck	Multiple punctiform abnormal intake foci on the left lateral neck	Abnormal intake foci on the left lateral neck, considered to be lymph node metastasis
6	F	32	Thyroid papillary (follicular carcinoma variant)	Multiple punctiform radioactive concentration areas on the mediastinum and bilateral chest	Multiple punctiform abnormal intake foci on the mediastinum and bilateral chest	Abnormal intake foci on the mediastinum and lungs, considered to be lymph node metastasis and lung metastasis
7	F	19	Thyroid papillary carcinoma	Multiple punctiform radioactive concentration areas on the bilateral chest	Multiple punctiform abnormal intake foci on the bilateral chest	Abnormal intake foci in the lungs, considered to be multiple lung metastases
8	F	53	Thyroid follicular carcinoma	Multiple punctiform radioactive concentration areas on the bilateral chest	Multiple punctiform abnormal intake foci on the bilateral chest	Abnormal intake foci on the, considered to be multiple lung metastases
9	F	56	Thyroid follicular carcinoma	Multiple punctiform radioactive concentration areas on the neck, upper mediastinum, and bilateral chest	Multiple punctiform abnormal intake foci on the neck, mediastinum, and bilateral chest	Abnormal intake foci on the neck, mediastinum, and lungs, considered to be neck lymph node, upper mediastinal lymph node, and multiple lung metastases
10	F	59	Thyroid papillary (follicular carcinoma variant)	Multiple punctiform and irregular radioactive concentration areas on the anterior cervical area	One lumpy abnormal intake focus on the anterior cervical area	Abnormal intake foci on the C7 vertebra, considered to be bone metastasis

Representative typical images

The typical image criteria were defined as clear functional imaging and clear positioning of the fault image, with representative lymph node, bone, or lung metastasis. The image selection only considers factors related to image quality, and not variables related to clinical staging, pathology, age, sex, and other factors.

Typical case 1 was a 56 y old woman diagnosed with thyroid follicular cancer. Thyroid static imaging before the ^{131}I treatment revealed multiple nodular areas of radioactive concentration in the neck, upper mediastinum, and bilateral thorax, resulting in a diagnosis of cervical and mediastinum lymph node metastases, along with bilateral lung metastases (Figure 1A). The patient was confirmed to have lymph node and lung metastases of thyroid follicular carcinoma by $^{99m}TcO_4^-$ cervical SPECT/CT fusion imaging, ^{131}I-WBS, and ^{131}I cervical/thoracic SPECT/CT fusion imaging (Figure 1D).

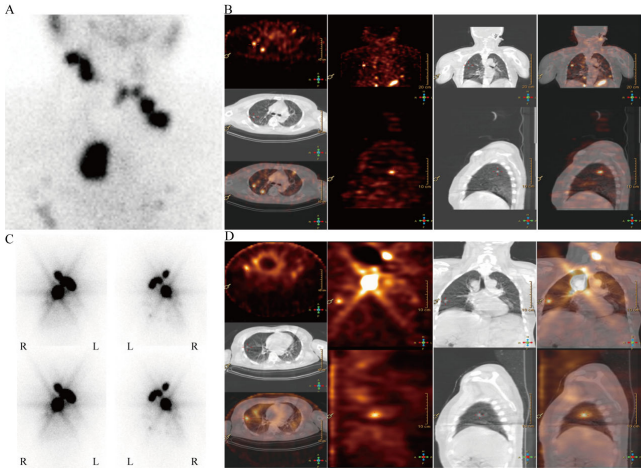

Figure 1. *Typical case 1, female, 56 y old, diagnosed as thyroid follicular cancer, cervical and mediastinum lymph nodule metastasis, bilateral lung metastasis. A: $^{99m}TcO_4^-$ cervical SPECT/CT fusion imaging: multiple nodular radioactive concentration areas in the neck, upper mediastinum, and bilateral thoraces; B: ^{131}I cervical/thoracic SPECT/CT fusion imaging: multiple nodular radioactive concentration areas in the neck, upper mediastinum, and bilateral lungs; C: ^{131}I whole body imaging: multiple nodular abnormal I intake foci in the neck, upper mediastinum, and bilateral thoraces; D: ^{131}I cervical/thoracic SPECT/CT fusion imaging: multiple abnormal I intake foci in the neck, upper mediastinum, and bilateral lungs, so the patient was diagnosed as cervical lymph node metastasis, upper mediastinal lymph node metastasis, and multiple metastases in the bilateral lungs.*

Typical case 2 was a 59 y old woman diagnosed with the follicular variant of papillary thyroid carcinoma. Thyroid static imaging before the ^{131}I treatment revealed punctate and irregular areas of radioactive concentration; these areas represented the residual thyroid tissue, as well as possible bone metastases (Figure 2A). The punctate areas of radioactive concentration were confirmed as residual thyroid tissue and the irregular areas of radioactive concentration were confirmed as cervical metastasis of the follicular variant of papillary thyroid carcinoma by $^{99m}TcO_4^-$ cervical SPECT/CT fusion imaging, ^{131}I-WBS, and ^{131}I cervical/thoracic SPECT/CT fusion imaging (Figures 2B-2D).

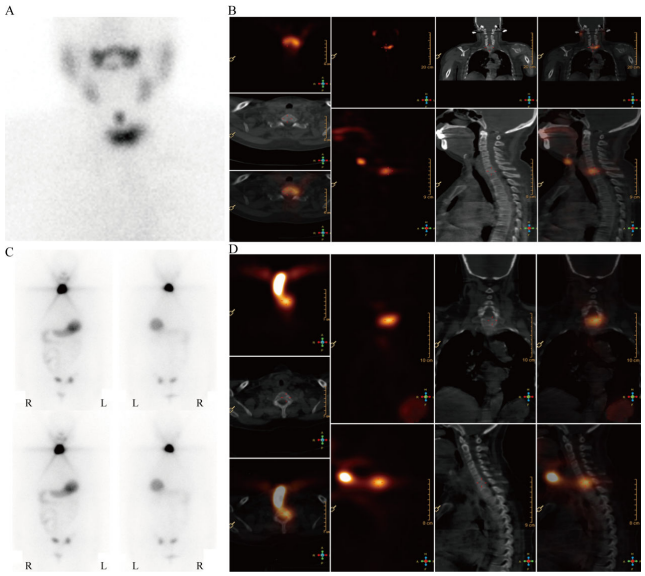

Figure 2. *Typical case 2, female, 59 y old, diagnosed as follicular variant of papillary thyroid carcinoma: C7 vertebral bone metastasis. A: $^{99m}TcO_4^-$ thyroid static imaging: punctate and irregular radioactive concentration areas anterior to the neck; B: $^{99m}TcO_4^-$ cervical/thoracic SPECT/CT fusion imaging: punctate radioactive concentration areas in the thyroid gland anterior to the neck; C: ^{131}I whole body imaging: one clump abnormal I intake focus; D: ^{131}I SPECT/CT fusion imaging: the abnormal I intake focus before the neck is the residual thyroid tissue; the abnormal I intake at C7 vertebral body is considered as bone metastasis.*

Discussion

Normal thyroid tissue has the NIS-mediated ability to perform selective uptake and accumulation of iodine. The elements Tc and iodine belong to the same family, and $^{99m}TcO_4^-$ is very similar to the inorganic iodine ion; thus, thyroid tissue can also take up and concentrate Tc. However, $^{99m}TcO_4^-$ cannot undergo further metabolism after it enters the thyroid cells, nor can it participate in the synthesis of thyroid hormones; hence, it can only reflect the uptake function of thyroid cells and not the metabolic function of iodine. The use of $^{99m}TcO_4^-$ has a long history in the diagnosis of thyroid disease due to its valuable imaging features. Currently, $^{99m}TcO_4^-$ is clinically used for thyroid static imaging to visualize the location, shape, size, and functional status of the thyroid.

Thyroid cancer is the most common endocrine system malignancy, accounting for 1.1% of systemic malignancies [14]. In recent years, a continued increase in the incidence of thyroid cancer has been observed, among which more than 90% of cases are DTC [15]. Cervical lymph node metastasis of DTC is common, and the most common locations of distant metastasis are the lungs and bone. Membrane expression of NIS is decreased in thyroid cancer cells. Therefore, in most preoperative routine thyroid static imaging studies, the cancer tissue shows a "cooled node" or "cold node," indicating reduced $^{99m}TcO_4^-$ uptake. When the normal thyroid tissue has

not been completely removed, metastatic lesions that concentrate $^{99m}TcO_4^-$ are rare. Only a small number of cervical lymph node metastases with $^{99m}TcO_4^-$ concentration have been reported in China, and no case of DTC with multiple metastatic lesions revealed by $^{99m}TcO_4^-$ thyroid static imaging has been reported. Further, only a few cases describing the uptake of Tc by thyroid cancer tissue have been reported in other countries [16-18]. Highly-differentiated DTC has a function similar to that of normal thyroid tissue. Therefore, $^{99m}TcO_4^-$ may also be taken up by highly-differentiated thyroid cancer and its metastatic lesions.

The results of this study showed that the sensitivity of $^{99m}TcO_4^-$ thyroid static imaging was 85.2%, exhibiting good consistency with postoperative ^{131}I-WBS (with a coincidence rate of 85.48%), similar to the findings of a prospective study by Khammash et al. that examined 66 patients with residual thyroid tissue after thyroid cancer resection [19]. The study of Ozdemir et al. [20] further showed that, compared with the standard of ^{131}I-WBS after treatment, the sensitivity, specificity, and positive predictive value of $^{99m}TcO_4^-$ thyroid static imaging were 72.2%, 70.5%, and 97.4%, respectively, and the authors thus concluded that $^{99m}TcO_4^-$ static thyroid imaging was very effective in assessing residual thyroid tissue and that it was helpful to determine the proper dose of ^{131}I treatment, which was consistent with the results of the presents study. The benefits of $^{99m}TcO_4^-$ thyroid static imaging include that it can accurately assess the status of the residual thyroid tissue, that it can be used to determine therapeutic doses to avoid the "stunning" phenomenon, and that it involves low radiation exposure for patients and medical staff.

Seventy-eight of the 420 patients enrolled in the present study had negative results on $^{99m}TcO_4^-$ thyroid static imaging but positive results on ^{131}I-WBS. These false negative results may be caused by smaller amounts of residual thyroid tissue with a relatively high background of thyroid bed area and surrounding tissue. On the other hand, this study found no false negative cases on ^{131}I-WBS, thus confirming that ^{131}I-WBS has a higher sensitivity and can be used as the gold standard for imaging thyroid tissue and metastatic lesions. Seven patients exhibited negative results on both imaging methods, an outcome that may be caused by more thorough thyroidectomy and subsequent lack of thyroid tissue residue. Based on the results of this study, we conclude that positive results on $^{99m}TcO_4^-$ thyroid static imaging can confirm the presence of residual thyroid tissue, whereas negative results cannot conclusively confirm its absence.

Furthermore, $^{99m}TcO_4^-$ thyroid static imaging also revealed some metastatic lesions when used for assessment of the residual thyroid tissue prior to ^{131}I therapy in this study. In our patients, SPECT planar imaging had been performed previously; as a result, uptake of the thyroid bed region was found on both imaging studies. If any abnormal uptake was found outside the thyroid, SPECT/CT fusion imaging was subsequently performed to determine the location and nature of the foci. The abnormal uptake of $^{99m}TcO_4^-$ outside the thyroid bed area has been previously reported to be more likely to be caused by lesion metastasis [13], especially in cases of bilateral lung uptake and bone uptake. Herein, the 10 patients with abnormal areas of $^{99m}TcO_4^-$ concentration outside the thyroid bed were confirmed to have lymph node, lung, or bone metastases by ^{131}I-WBS, SPECT/CT fusion imaging, or ultrasound (Table 2).

Our detailed analysis of the above-mentioned 10 cases further confirmed that some DTC metastases were well-differentiated and showed higher expression of NIS, indicating that they can readily take up and concentrate $^{99m}TcO_4$ and ^{131}I; these characteristics are more common in thyroid follicular carcinoma and thyroid follicular papillary carcinoma. Some studies have shown that the application of $^{99m}TcO_4^-$ WBS combined with SPECT/CT imaging plays a useful role in detecting metastatic lesions of DTC in the neck and chest [13]. Byeong's study revealed that high levels of TSH under stimulation conditions may improve the diagnostic capacity of thyroid static imaging for detecting metastatic lesions of DTC [12].

In this study, thyroid static imaging was performed under stimulation conditions (TSH>30 μIU/ml), demonstrating that it can identify metastatic lesions in certain cases of DTC, potentially associated with high TSH levels. The reason that $^{99m}TcO_4^-$ thyroid static imaging can reveal metastases of DTC may be related to the fact that metastases have higher NIS expression and a higher degree of differentiation, suggesting that they have high ^{131}I uptake ability, as well as good susceptibility to ^{131}I treatment and thus a better prognosis.

Following observation of the therapeutic effect of ^{131}I in clinical work and the identification of metastatic lesions of DTC by $^{99m}TcO_4^-$ thyroid static imaging, the therapeutic effect of ^{131}I has been well verified. However, its prognostic ability requires long-term follow-up for verification. Further, the results of our analysis still require confirmation through pathological analysis of the metastatic lesions.

The use of $^{99m}TcO_4^-$ thyroid static imaging can help initially determine the differentiation status of metastatic lesions and identify some metastatic lesions, thus providing better guidance for the selection of therapeutic doses. As ^{131}I treatment protocols are established based on the presence of metastases as well as their location, accurately identifying the number, location, and iodine uptake function of the metastatic lesions of thyroid cancer will have great significance in the decision-making regarding the patients' treatment [21]. Especially, $^{99m}TcO_4^-$ thyroid static imaging is useful for assessing the size, location, and function of residual thyroid tissue before post-DTC ^{131}I treatment and for suggesting individualized treatment of DTC patients, as compared to ^{131}I imaging. Hence, it should be widely used in the clinical setting. As mentioned above, in the present study, 10 patients with DTC metastases were identified by $^{99m}TcO_4^-$ thyroid static imaging, which provided useful information for the treatment of these patients. Moreover, in some cases, the results were used to adjust the patients' clinical stages and treatment plans and to predict the efficacy and prognosis of ^{131}I treatment;

thus, the procedure has some utility in guiding individualized DTC treatment.

There are some limitations in this study. Although $^{99m}TcO_4^-$ thyroid static imaging may be used to suggest the subsequent treatment of DTC patients, pathological examination of the expression of NIS in metastatic lesions and analysis of long-term follow-up data were not conducted; these data will be collected and reported in the future. Further, owing to limitations in the sample size and follow-up time, only partial conclusions can be drawn, and some conclusions are only speculations. The outcomes of the study patients need to be further followed-up for a long time.

In conclusion, $^{99m}TcO_4^-$ thyroid static imaging can identify metastatic lesions of DTC, and we speculate that the uptake principle is related to the high expression of NIS and the higher degree of differentiation of these lesions. However, this hypothesis requires further confirmation by pathological examination of the metastatic lesions.

Conflicts of Interest

The authors declare no conflict of interest.

References

1. Haugen BR, Alexander EK, Bible KC, Doherty GM, Mandel SJ, Nikiforov YE, Pacini F, Randolph GW, Sawka AM, Schlumberger M, Schuff KG, Sherman SI, Sosa JA, Steward DL, Tuttle RM, Wartofsky L. 2015 American thyroid association management guidelines for adult patients with thyroid nodules and differentiated thyroid cancer: the american thyroid association guidelines task force on thyroid nodules and differentiated thyroid cancer. Thyroid 2016; 26: 1-133.
2. Hilditch TE, Dempsey MF, Bolster AA, McMenemin RM, Reed NS. Self-stunning in thyroid ablation: evidence from comparative studies of diagnostic 131I and 123I. Eur J Nucl Med Mol Imaging 2002; 29: 783-788.
3. Lassmann M, Luster M, Hanscheid H, Reiners C. Impact of 131I diagnostic activities on the biokinetics of thyroid remnants. J Nucl Med 2004; 45: 619-625.
4. Silberstein EB. Comparison of outcomes after (123)I versus (131)I pre-ablation imaging before radioiodine ablation in differentiated thyroid carcinoma. J Nucl Med 2007; 48: 1043-1046.
5. Amdur R, Mazzaferri E. Thyroid stunning. Essentials of thyroid cancer management. US Springer 2005; 55-59.
6. Morris LF, Waxman AD, Braunstein GD. The nonimpact of thyroid stunning: remnant ablation rates in 131I-scanned and nonscanned individuals. J Clin Endocrinol Metab 2001; 86: 3507-3511.
7. Dam HQ, Kim SM, Lin HC, Intenzo CM. 131I therapeutic efficacy is not influenced by stunning after diagnostic whole-body scanning. Radiology 2004; 232: 527-533.
8. Kim CY, Jeong SY, Lee SW, Lee J, Ahn BC. Scintigraphic demonstrations of a retrosternal goiter. Rev Esp Med Nucl Imagen Mol 2014; 33: 183-184.
9. Ahn BC. Retrosternal goiter visualized on 99mTc pertechnetate SPECT/CT, but not on planar scintigraphy. Clin Nucl Med 2016; 41: 169-170.
10. Mathiopoulou L, Chrisoulidou A, Boudina M, Mitsakis P, Mandanas S, Pazaitou-Panayiotou K. 99mTc pertechnetate thyroid scan leads to serendipitous detection of metastatic thyroid cancer. Clin Nucl Med 2012; 37: 604-606.
11. Oh JR, Ahn BC, Jeong SY, Lee SW, Lee J. Radioiodine scan index: a simplified, quantitative treatment response parameter for metastatic thyroid carcinoma. Nucl Med Mol Imaging 2015; 49: 174-181.
12. Ahn BC. Reinforcing the ability of 99mTcO4 scintigraphy for identifying differentiated thyroid cancer by TSH stimulation. Clin Nucl Med 2016; 41: 412-413.
13. Chantadisai M, Kingpetch K. Usefulness of (99m) Tc-pertechnetate whole body scan with neck and chest SPECT/CT for detection of post-surgical thyroid remnant and metastasis in differentiated thyroid cancer patients. Ann Nucl Med 2014; 28: 674-682.
14. Chen W, Zheng R, Zuo T, Zeng H, Zhang S, He J. National cancer incidence and mortality in China, 2012. Chin J Cancer Res 2016; 28: 1-11.
15. Sherman SI. Thyroid carcinoma. Lancet 2003; 361: 501-511.
16. Carr HA, Temple TE, Staab EV. Early visualization of 99mTc-pertechnetate in metastatic thyroid cancer in a patient with Graves disease. J Nucl Med 1971; 12: 40-42.
17. Scott GC, Meier DA, Dickinson CZ. Cervical lymph node metastasis of thyroid papillary carcinoma imaged with fluorine-18-FDG, technetium-99m-pertechnetate and iodine-131-sodium iodide. J Nucl Med 1995; 36: 1843-1845.
18. Verma N, Singh-Wadhwa S, Arvela OM. Metastatic thyroid cancer visualized on technetium pertechnetate and iodine-131 scintigraphy. Clin Nucl Med 2002; 27: 610.
19. Khammash NF, Halkar RK, Abdel-Dayem HM. The use of technetium-99m pertechnetate in postoperative thyroid carcinoma. A comparative study with iodine-131. Clin Nucl Med 1988; 13: 17-22.
20. Ozdemir D, Cuhaci FN, Ozdemir E, Aydin C, Ersoy R, Turkolmez S, Cakir B. The role of postoperative Tc-99m pertechnetate scintigraphy in estimation of remnant mass and prediction of successful ablation in patients with differentiated thyroid cancer. Nucl Med Commun 2016; 37: 640-645.
21. Tsai CJ, Cheng CY, Shen DH, Kuo SJ, Wang LY, Lee CH, Wang JJ, Chang MC, Huang WS. Tc-99m imaging in thyroidectomized differentiated thyroid cancer patients immediately before I-131 treatment. Nucl Med Commun 2016; 37: 182-187.

***Correspondence to**

Xiaoyong Zhang

Department of Radionuclide Treatment Center

Beijing 401 Hospital of Chinese Nuclear Industry

PR China